

# Fold of a bifurcation solution from the figure-eight choreography in the three body problem

Hiroshi Fukuda

*Colledge of liberal arts and sciences, Kitasato University, Kitasato 1-15-1  
 Minami-ku, Sagamihara-shi, Kanagawa 252-0373, Japan  
 fukuda@kitasato-u.ac.jp*

Hiroshi Ozaki

*STEM Education Center, Tokai University, 4-1-1, Kitakaname  
 Hiratsuka, Kanagawa 259-1292, Japan  
 ozaki@tokai.ac.jp*

Received (Month Day Year); Accepted (Month Day Year); Published (Month Day Year)

In the figure-eight choreography in the classical three-body problem, both side bifurcation solutions sometimes fold at one side of the bifurcation point with cusp of action. Three numerical examples of such fold for figure-eight choreography under the Lennard-Jones-type potential and one under the homogeneous potential are introduced. Up to the forth order of representation variable of the Lyapunov-Schmidt reduced action in two dimension with three-fold symmetry, the fold is analyzed.

*Keywords:* bifurcation, three-body, cusp, figure-eight, choreography, Lyapunov-Schmidt

## 1. Introduction

The figure-eight choreography in the three-body problem is a motion of three equal masses in classical mechanics, chasing each other in the common figure-eight-shaped orbit [Moore, 1993; Chenciner, 2000]. Sometimes equivariant bifurcations [Chossat, P. & Lauterbach] occur loosing its symmetries partially from its full symmetry elements forming a crystallographic point group [Chenciner, 2005]. Under the inhomogeneous interaction potential such as the Lennard-Jones-type (hereafter LJ) potential [Sbano, 2004, 2010; Fukuda *et al.*, 2017], it bifurcates by the period  $T$  of the motion as bifurcation parameter [Fukuda *et al.*, 2019]. For the homogeneous interaction potential, bifurcations occur by the power of the homogeneous potential [Fukuda *et al.*, 2019] or one of the masses of the bodies [Galán *et al.*, 2002; Doedel *et al.*, 2003].

We notice that some bifurcation solution soon folds as a function of bifurcation parameter [Fukuda *et al.*, 2019; Fukuda & Ozaki, 2025]. In this paper, the fold is analyzed using the Lyapunov-Schmidt (hereafter LS) reduced action in two dimension up to the forth order of its representation variable in case the bifurcation parameter does not change the symmetry of Lagrangian. The period of motion and the power of the homogeneous potential does not change the symmetry of Lagrangian while does one of the masses in the equal mass three bodies.

In section 2, three-fold-type bifurcation and its LS reduced action into two dimensional representation are introduced according to our previous paper [Fukuda & Ozaki, 2025]. In section 2.2, variational equations for the LS reduced action are solved up to the forth order of the two dimensional representation variables. It is shown that the bifurcation solutions fold under a condition given by the third and forth expansion

coefficients. In section 2.3, the LS reduced action in two dimension is displayed by three dimensional plot, and the relations among solutions are recognized as those among critical points visually. In section 2.4, the third and forth order expansion coefficient are given by time integral of the third and forth order differentiation in generalized coordinates of the Lagrangian, respectively. In section 3, four numerical examples in figure-eight choreography under the homogeneous and inhomogeneous LJ potential are shown. Section 4 is the summary and discussions.

## 2. Three-fold-type Bifurcation

### 2.1. Definition

A necessary condition of bifurcation for a periodic solution  $q(t)$  with a period  $T$ ,  $q(t) = q(t + T)$ , of the Euler-Lagrange equations

$$\frac{d}{dt} \frac{\partial L}{\partial \dot{q}} = \frac{\partial L}{\partial q} \quad (1)$$

for the Lagrangian

$$L = \frac{1}{2} \dot{q}^2 - U \quad (2)$$

of three-body system where

$$U = \sum_{i>j} u(r_{ij}) \quad (3)$$

is an interaction potential and  $r_{ij}$  a distance between body  $i$  and  $j$ , is that the eigenvalue  $\kappa$  of a Hessian operator [Fukuda *et al.*, 2019]

$$H(q) = -\frac{d^2}{dt^2} + \frac{\partial^2}{\partial q^2} L(q, \dot{q}) \quad (4)$$

crosses zero. The generalized coordinate  $q$  is a nine dimensional real vector

$$q = (q_1, q_2, \dots, q_9) = (x_1, y_1, z_1, x_2, y_2, z_2, x_3, y_3, z_3) \quad (5)$$

composed of position vectors  $(x_i, y_i, z_i)$  of body  $i$ . We use the matrix notation, however, we do not distinguish column and row vectors strictly if it is obvious from the context.

In the vicinity of the bifurcation point, according to the degeneracy  $d$  of the eigenvalue  $\kappa$ , action

$$S(q) = \int_0^T L(q) dt \quad (6)$$

is represented in  $d$  dimension by LS reduction

$$S(r_1, r_2, \dots, r_d) = S(q). \quad (7)$$

The  $d$  dimensional real column vector  $r = {}^t(r_1, r_2, \dots, r_d)$  is a representation of  $d$  degenerate real orthonormalized eigenfunction

$$\phi = (\phi_1, \phi_2, \dots, \phi_d) \quad (8)$$

with

$$\int_0^T {}^t \phi_i \phi_j dt = \delta_{ij} \quad (9)$$

of eigenvalue  $\kappa$

$$H(q) \phi_i = \kappa \phi_i \quad (10)$$

as  $\phi r$ , where  $\delta_{ij}$  is the Kronecker delta and  ${}^t$  transpose.

Suppose  $G(q) = \{g | gH(q) = H(q)\}$  is a finite isotropy subgroup of operators acting on  $H(q)$  and  $D(g)$  is a  $d$  dimensional real representation of  $g \in G(q)$  in the eigenspace of  $\kappa$  spanned by  $\phi$ . If  $S = Sg$  for all  $g \in G(q)$ ,  $S(r)$  has a symmetry

$$S(r) = S(D(g)r) \quad (11)$$

and bifurcations are classified by the group  $D(q) = \{D(g) | g \in G(q)\}$ . If the group  $D(q)$  is isomorphic to  $C_3$  or  $D_3$  where  $C_n$  and  $D_n$  are the cyclic and dihedral group of order  $n$ , respectively, the bifurcation is classified to the three-fold-type.

For three-fold-type bifurcation, the LS reduced action is expanded under restriction (11) as

$$S(r, \theta) = S(q) + \frac{\kappa}{2}r^2 + \frac{A_3}{3!}r^3 \sin(3\theta) + \frac{A_4}{4!}r^4 + \dots \quad (12)$$

where  $r_1 = r \cos \theta$  and  $r_2 = r \sin \theta$ . The Euler-Lagrange equations are then rewritten by variational principle in  $r$  and  $\theta$ ,

$$\begin{aligned} \frac{\partial}{\partial \theta} S(r, \theta) &= \frac{A_3}{2!}r^3 \cos(3\theta) + \dots = 0, \\ \frac{\partial}{\partial r} S(r, \theta) &= \kappa r + \frac{A_3}{2!}r^2 \sin(3\theta) + \frac{A_4}{3!}r^3 + \dots = 0. \end{aligned} \quad (13)$$

We suppose the coefficient  $A_3 \neq 0$  and  $A_4 \neq 0$ .

## 2.2. Solutions up to the forth order

The variational principle (13) gives solution  $r = 0$  representing  $q$  and three solutions

$$(r, \theta) = (r_-(\kappa), \theta_n), \quad n = 1, 2, 3, \quad (14)$$

and the other three solutions

$$(r, \theta) = (r_+(\kappa), \theta_n), \quad n = 1, 2, 3, \quad (15)$$

may exist, where

$$r_{\pm}(\kappa) = \frac{1}{2} \left( \left| \frac{3A_3}{A_4} \right| \pm \sqrt{\left( \frac{3A_3}{A_4} \right)^2 - \frac{24\kappa}{A_4}} \right), \quad (16)$$

$$\theta_n = \begin{cases} \frac{\pi}{6} + \frac{2n\pi}{3}, & (A_3 A_4 < 0), \\ \frac{\pi}{6} + \frac{(2n+1)\pi}{3}, & (A_3 A_4 > 0). \end{cases} \quad (17)$$

The three solutions (14) exist for  $|r_-(\kappa)| \ll 1$  independent of sign of  $\kappa$  and go to  $r_-(\kappa) \rightarrow 0$  for  $\kappa \rightarrow 0$  thus they are bifurcation solutions and bifurcation is both sides. On the other hand, though the other three solutions (15) may exist also in the both sides, they do not go to  $q$  for  $\kappa \rightarrow 0$  since  $r_+(\kappa) \rightarrow |3A_3/A_4| \neq 0$  for  $\kappa \rightarrow 0$ . Thus they are not direct bifurcation solutions but fold solutions at

$$\kappa = \kappa_0 = \frac{3A_3^2}{8A_4}, \quad (18)$$

where two sets of three solutions (14) and (15) coincide:

$$\{r_-(\kappa_0)(\cos \theta_n, \sin \theta_n) | n = 1, 2, 3\} = \{r_+(\kappa_0)(\cos \theta_n, \sin \theta_n) | n = 1, 2, 3\}$$

in order  $|r_{\pm}(\kappa_0)|^4$ . At the fold point (18), if

$$r_0 = |r_{\pm}(\kappa_0)| = \left| \frac{3A_3}{2A_4} \right| \quad (19)$$

is enough smaller than 1, the fold solution (15) is expected to exist.

The relative actions  $\Delta S_{\pm}(\kappa) = S(r, \theta) - S(q)$  obtained by the substitution of (14) and (15) into (12) for the bifurcation solution with minus subscript and for the fold solution with plus subscript,

$$\Delta S_{\pm}(\kappa) = \frac{\kappa}{2} r_{\pm}^2(\kappa) - \frac{|A_3|}{3!} \frac{A_4}{|A_4|} r_{\pm}^3(\kappa) + \frac{A_4}{4!} r_{\pm}^4(\kappa) + \dots, \quad (20)$$

behave like curves in Fig. 1 for  $A_3 = 0.518$  and  $A_4 = -8.40$ . The cusp at  $\kappa = \kappa_0$  where  $\Delta S_{-}(\kappa) = \Delta S_{+}(\kappa) = \Delta S_0$  with

$$\Delta S_0 = \Delta S_{\pm}(\kappa_0) = \frac{9A_3^4}{128A_4^3} \quad (21)$$

is the fold point and  $\Delta S_{-}(0) = 0$  but  $\Delta S_{+}(0) = -9A_3^4/(8A_4^3) \neq 0$ . It is the ordinary cusp

$$\Delta S_{\pm}(\kappa) = \mp \frac{|A_3|}{48} \frac{A_4}{|A_4|} k^{3/2} + \frac{A_4}{64} \left( \frac{9A_3^4}{2A_4^4} - \frac{3A_3^2}{A_4^2} k - \frac{1}{6} k^2 + \dots \right), \quad (22)$$

on the smooth curve of  $\kappa$  in the second term at the right hand side of (22), where  $k = 24(\kappa_0 - \kappa)/A_4$ .

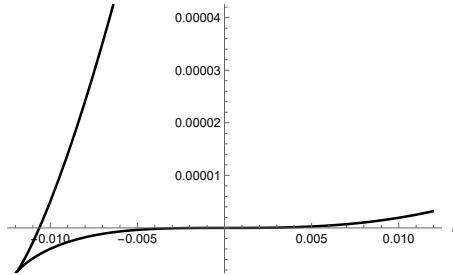


Fig. 1.  $\Delta S_{\pm}(\kappa)$  for  $A'_3 = 0.518$  and  $A_4^{(0)} = -8.40$ .

### 2.3. Graphical Explanation

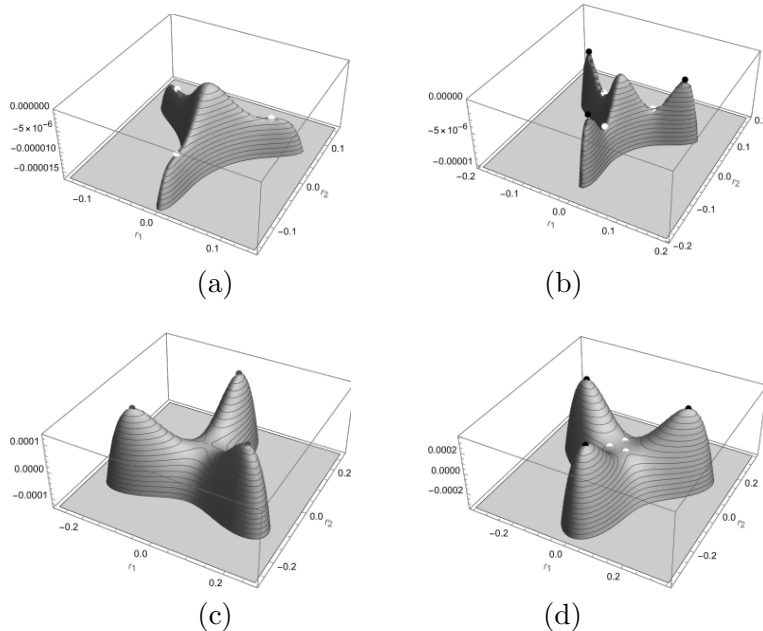


Fig. 2.  $\Delta S(r_1, r_2)$  for  $A_3 = 0.518, A_4 = -8.40$ . (a)  $\kappa = \kappa_0 = -0.012$ . (b)  $\kappa = 0.9\kappa_0$ . (c)  $\kappa = 0$ . (d)  $\kappa = -0.9\kappa_0$ . In (a)–(d), white points represent bifurcation solutions and black fold solutions. Mountain or pond at the center represents solution  $q$ .

In Fig. 2, the three-dimensional plot for  $\Delta S(r_1, r_2) = S(r, \theta) - S(q)$  in  $(r_1, r_2)$ -plane with  $A_3 = 0.518$ ,  $A_4 = -8.40$  is shown to explain the seven solutions including  $q$  visually. In Figs. 2 (a)–(d), mountain or pond at center correspond to  $q$ .

Fig. 2 (a) shows  $\Delta S(r_1, r_2)$  at  $\kappa = \kappa_0 < 0$ . Three mountains with white points around the center mountain are the three bifurcation solutions at the fold point.

Fig. 2 (b) shows  $\Delta S(r_1, r_2)$  for  $\kappa_0 < \kappa < 0$ . Three mountains with black point are solutions from fold points which do not go to the center  $q$ , we called them fold solutions. Three saddles with white points between center mountain representing  $q$  and fold solutions are bifurcation solutions towards the solution  $q$ , we called them simply bifurcation solutions.

Fig. 2 (c) shows  $\Delta S(r_1, r_2)$  for  $\kappa = 0$  that is the bifurcation point, where three bifurcation solutions with white points merge into one at center representing  $q$ .

Fig. 2 (d) shows  $\Delta S(r_1, r_2)$  for  $\kappa > 0$  where three bifurcation solutions with white points are placed at the opposite side of fold solutions with black points from the center  $q$ .

It is seen that three mountains with black points are located in the almost same place and three saddles with white points start moving from the three mountains with black points and are moving towards the center  $q$  then to the opposite sides.

## 2.4. Integral Expression of the Coefficients

The coefficient  $A_3$  in (12) is given by expansion of action around  $q$  [Fujiwara *et al.*, 2020] as

$$A_3 = \begin{cases} A_3^{(0)}, & (D(q) = D_3) \\ \frac{1}{3}\sqrt{(A_3^{(1)})^2 + (3A_3^{(0)})^2}, & (D(q) = C_3) \end{cases} \quad (23)$$

with

$$A_3^{(j)} = \binom{3}{j} \int_0^T dt (\phi_1 \frac{\partial}{\partial q})^j (\phi_2 \frac{\partial}{\partial q})^{3-j} L, \quad (24)$$

where  $\phi_2$  is more symmetric eigenfunction than  $\phi_1$  for  $D(q) = D_3$ . (24) is numerically calculable by integrated symbolic and numerical computing system such as Mathematica [Wolfram Research Inc., 2024].

On the other hand,  $A_4$  is given by all eigenfunctions  $\psi_i$  of  $H(q)$  with non zero eigenvalue  $\lambda_i \neq 0$  at bifurcation point as

$$A_4 = \int_0^T dt (\phi_2 \frac{\partial}{\partial q})^4 L - 3 \sum_i \frac{1}{\lambda_i} \int_0^T dt (\psi_i \frac{\partial}{\partial q} (\phi_2 \frac{\partial}{\partial q})^2)^2 L. \quad (25)$$

(25) is not numerically calculable without further manipulation of expression since infinitely many eigenfunctions  $\psi_i$  are contained.

## 3. Numerical Calculations

In our numerical calculations published [Fukuda *et al.*, 2019; Fukuda & Ozaki, 2025], there are four three fold type bifurcations shown in table 1.

In table 1, the first column shows the original periodic solution  $q$ .  $\alpha_{\pm}$  are the figure-eight choreography under the LJ potential

$$u(r) = \frac{1}{r^{12}} - \frac{1}{r^6}. \quad (26)$$

The action for  $\alpha_+$  is higher than  $\alpha_-$  at the same period  $T$  and they coincide at minimum  $T = 14.479$  [Fukuda *et al.*, 2017].  $C_y$  is the figure-eight shaped choreographic solution bifurcated at  $T = 17.132$  from  $\alpha_+$  which is symmetric in  $y$ -axis but not in  $x$ -axis [Fukuda *et al.*, 2019]. ‘ $\infty$ ’ is the figure-eight choreography under the homogeneous potential

$$u(r) = -\frac{1}{ar^a} \quad (27)$$

Table 1. Numerical results.

$q$	bifurcation point	fold point	$\kappa_0$	$\Delta S_0$	$A_3$	(23)	$A_4$	$r_0$
$\alpha_+$	$T = 16.878$	16.875	$+6.6 \times 10^{-5}$	$+3.0 \times 10^{-9}$	0.011	0.011	0.736	0.023
$\alpha_-$	$T = 14.836$	14.797	$-1.2 \times 10^{-2}$	$-8.5 \times 10^{-6}$	0.544	0.466	-8.97	0.091
$C_y$ <sup>a)</sup>	$T = 17.235$	17.234	$-2.4 \times 10^{-4}$	$-5.1 \times 10^{-9}$	0.059	0.056	-5.49	0.016
$\infty$ <sup>b)</sup>	$a = 0.9966$	1.027	$+1.5 \times 10^{-2}$	$+3.8 \times 10^{-3}$	0.036	0.037	0.031	1.719

<sup>a)</sup> Choreographic solution symmetric in  $y$  axis bifurcated from  $\alpha_+$  at  $T = 17.132$  [Fukuda *et al.*, 2019].

<sup>b)</sup> Homogeneous figure eight [Fukuda *et al.*, 2019],  $T = 2\pi$

with period  $T = 2\pi$ .

The bifurcation point is shown in the second column with bifurcation parameter  $T$  or  $a$ . The third column shows a fold point in the bifurcation parameter where fold of bifurcation solution occurs. The forth and fifth columns show  $\kappa_0$  and  $\Delta S_0$ , respectively.

In the sixth and eighth columns, values of  $A_3$  and  $A_4$  numerically calculated by solving coupled equations (18) and (21) using the numerical values tabulated in the forth and fifth columns are shown. These coefficients  $A_3$  and  $A_4$  are expected to be independent of  $\kappa$  and actually their figures in tables is not changed by  $\kappa$  in the vicinity of the bifurcation point,  $|\kappa| \ll 1$ .

On the other hand, in the seventh column  $A_3$  calculated by numerical integration (23) with (24) is shown. Here a relation

$$\kappa = \int_0^T dt (\phi_i \frac{\partial}{\partial q})^2 L, \quad i = 1, 2, \quad (28)$$

is useful to check the numerical integration (24). It is noted that the third example is the only case with  $D(q) = C_3$  among four examples. In this case, though there is no numerical way to fix  $\phi_2$ , numerically  $A_3$  does not depend on choice of  $\phi_2$ . For the other examples with  $D(q) = D_3$ ,  $\phi_2$  is chosen for parametric plot of  $q + h\phi_2$  by  $t$  showing higher symmetry. For all four examples,  $A_3$  fitted by using (18) and (21) in the sixth column is reasonably close to that by numerical integration (24) in the seventh column.

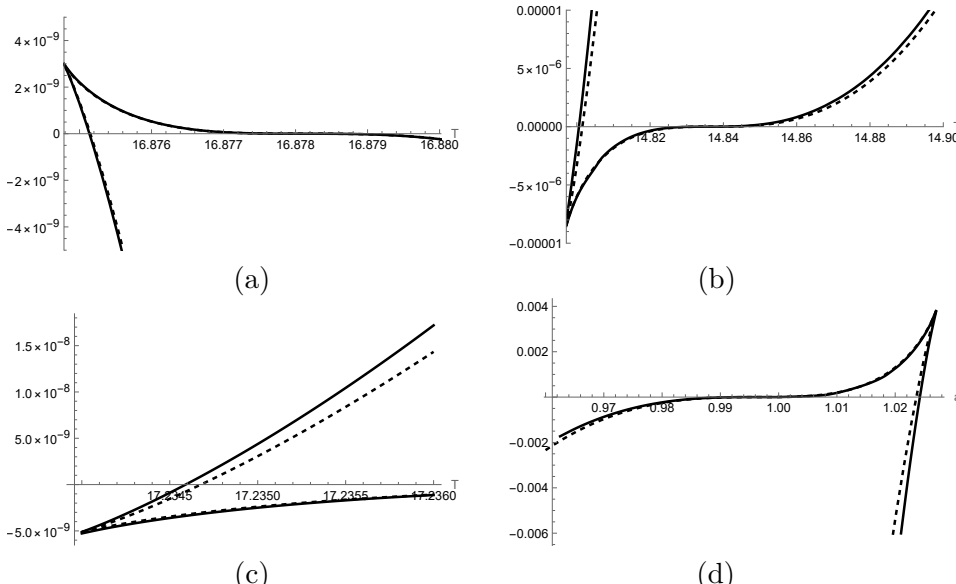


Fig. 3. (a)  $\Delta S_{\pm}(\kappa(T))$  for bifurcation at  $T = 16.878$  from  $\alpha_+$  under LJ potential (26).  $\kappa(T) = 0.336 - 0.0199T$ . (b)  $\Delta S_{\pm}(\kappa(T))$  for bifurcation at  $T = 14.836$  from  $\alpha_-$  under LJ potential (26).  $\kappa(T) = -4.59 + 0.309T$ . (c)  $\Delta S_{\pm}(\kappa(T))$  for bifurcation at  $T = 17.235$  from  $C_y$  bifurcated at  $T = 14.132$  from  $\alpha_+$  under LJ potential (26).  $\kappa(T) = -0.671 + 0.0389T$ . (d)  $\Delta S_{\pm}(\kappa(a))$  for bifurcation at  $a = 0.9966$  from figure-eight choreography under the homogeneous potential (27).  $\kappa(a) = -0.504 + 0.506a$ . In (a)–(d), solid curves are calculated by numerical exact bifurcation solutions and dashed by (20) using coefficients  $(A_3, A_4)$  in table 1 and the first order  $\kappa(T)$  or  $\kappa(a)$  around  $\kappa = 0$  above.

In the last column,  $r_0$  (19) at fold point is shown. Excepting the forth example for figure-eight under the homogeneous potential, the rest three are  $r_0 \ll 1$  then the fold should be explained by expansion (12). Actually, as plotted in Fig. 3 (a)–Fig. 3 (c),  $\Delta S_{\pm}(\kappa(T))$  calculated by (20) shown in dashed curve, using the coefficients ( $A_3, A_4$ ) in table 1 and the first order  $\kappa(T)$  around  $\kappa = 0$  in caption of Fig. 3 are close to those by numerical exact bifurcation solutions in solid curve.

For the fourth example, figure-eight under the homogeneous potential, as seen from Fig. 3 (d), though  $r_0 = 1.719 > 1$ ,  $\Delta S_{\pm}(\kappa(a))$  by (20) shown in dashed curve using the first order  $\kappa(a)$  around  $\kappa = 0$  given in caption of Fig. 3 is also close to that by numerical exact bifurcation solutions in solid curve. Note that this bifurcation solution is Simó's H solution [Simó, 2002] at  $a = 1$ , and becomes brake orbit like solution at  $a = 1$  after fold at  $a = 1.027$  [Fukuda *et al.*, 2019b]. In the opposite side, it bifurcates to non-planer solution at  $a = 0.846$  and finally folds at  $a = 0.8156$  [Fukuda *et al.*, 2020].

#### 4. Summary and discussions

It is shown that in figure-eight choreography and its bifurcation cascade solutions, both side bifurcation loosing symmetry will soon fold in one side as a function of bifurcation parameter if

$$\left| \frac{3A_3}{2A_4} \right| \ll 1 \quad (29)$$

and the bifurcation parameter does not change the symmetry of Lagrangian, since among four bifurcation types only the three-fold-type bifurcation is both side bifurcation loosing symmetry [Fukuda & Ozaki, 2025]. For bifurcation at  $a = 0.9966$  of the figure-eight choreography under the homogeneous potential (27) the condition (29) is not satisfied but fold occurs according to the analysis in section 2.4, which may show that the condition (29) is not so sensitive. As seen in section 2.3 visually, fold phenomenon may occur independent of the condition (29) since another mountain representing fold solution seems necessary to produce saddle point close to the summit of the mountain representing  $q$ .

Finally, fold phenomenon will occur in the general few body problem if the symmetry of Lagrangian is not changed by a bifurcation parameter and the bifurcation is described by the LS reduced action in two dimension with three fold symmetry.

#### References

Chenciner, A. & Montgomery, R. [2000] “A remarkable periodic solution of the three-body problem in the case of equal masses,” *Annals of Mathematics* **152**(3), 881–901.

Chenciner, A., Féjoz, J. & Montgomery, R. [2005] “Rotating Eights: I. The three  $\Gamma_i$  families,” *Nonlinearity* **18**, 1407–1424.

Chossat, P. & Lauterbach, R., [2000] “Methods in Equivariant Bifurcations and Dynamical Systems,” (World Scientific)

Doedel, E. J., Paffenroth, R. C., Keller, H. B., Dichmann, D. J. & Galán-Vioque, J. [2003] “Continuation of periodic solutions in conservative systems with application to the 3-body problem,” *International Journal of Bifurcation and Chaos* **13** No. 6, p. 1353–1381.

Fujiwara, T., Fukuda, H. & Ozaki, H. [2020] “Variational Principle of Action and Group Theory for Bifurcation of Figure-eight solutions,” *arXiv* 2002.03496v3 [math-ph]

Fukuda, H., Fujiwara, T. & Ozaki, H. [2017] “Figure-eight choreographies of the equal mass three-body problem with Lennard-Jones-type potentials,” *J. Phys. A: Math. Theor.* **50**, p. 105202.

Fukuda, H., Fujiwara, T. & Ozaki, H. [2018] “Morse index for figure-eight choreographies of the equal mass three-body problem,” *J. Phys. A: Math. Theor.* **51**, p. 145201.

Fukuda, H., Fujiwara, T. & Ozaki, H. [2019] “Morse index and bifurcation for figure-eight choreographies of the equal mass three-body problem,” *J. Phys. A: Math. Theor.* **52**, p. 185201.

Fukuda, H., Fujiwara, T. & Ozaki, H. [2019] “Bifurcation of Simó H solution bifurcated from figure-eight choreographies of the equal mass three-body problem,” *Symposium on Celestial Mechanics in Sagamihara*, <https://researchmap.jp/fukudahi/presentations/26949852>

## 8 Authors' Names

Fukuda, H., Fujiwara, T. & Ozaki, H. [2020] “Non-planer solution bifurcated from figure-eight choreography in equal mass three body problem,” *The Japan Society for Industrial and Applied Mathematics, Annual Meeting, Proceedings* pp. 252–253

Fukuda, H. & Ozaki, H. [2025] “Bifurcation analysis of figure-eight choreography in the three-body problem based on crystallographic point groups,” *J. Phys. A: Math. Theor.* **58**, p. 025203.

Galán, J., Muñoz-Almaraz, F. J., Freire, E., Doedel, E. & Vanderbauwhede, A. [2002] “Stability and Bifurcations of the Figure-8 Solution of the Three-Body Problem,” *Phys. Rev. Lett.* **88**, p. 241101-1–4.

Moore, C. [1993] “Braids in classical dynamics,” *Phys. Rev. Lett.* **70**, 3675–3679.

Sbano, L. [2004] “Symmetric solutions in molecular potentials,” *Symmetry and Perturbation Theory*, 291–299.

Sbano, L. & Southall, J. [2010] “Periodic solutions of the n-body problem with Lennard-Jones-type potentials,” *Dynamical Systems* **25**(1), 53–73.

Simó, C. [2002] “Dynamical properties of the figure eight solution of the three body problem,” *Contemporary mathematics* **292**, 209–228.

Wolfram Research Inc. [2024] “Mathematica, Version 14.2,” Champaign, IL